Symbol Error Rate Minimization Precoding for Interference Exploitation

Ka Lung Law, *Member, IEEE*, and Christos Masouros, *Senior Member, IEEE*

***Abstract*— This paper investigates a new beamforming approach for interference exploitation, which has recently attracted interest as an alternative to conventional interference-avoidance beamforming for the downlink of multiple-input multiple-output systems. Contrary to existing interference exploitation approaches that focus on signal-to-noise ratio performance, we adopt an approach based on the detection region of the signal constellation. Focusing on quality of service, we then formulate the optimization for minimizing the error probability (EP) for the worst user, subject to power constraints. We do this by employing the knowledge of channel state information at the transmitter, along with all downlink users' data that are readily available at the base station during downlink transmission. In this context, we also show that the detection-region-based beamforming and the worst user EP downlink beamforming are equivalent problems. Finally, we further propose a sum EPs approach and provide an analytic bound of average symbol error rate performance. Our simulations verify that the proposed techniques provide significantly improved performance over conventional downlink beamforming techniques.**

***Index Terms*— Downlink beamforming, error probability, convex optimization, constructive interference.**

I. Introduction

With the aid of channel state information (CSI) at the transmitter, downlink beamforming can serve multiple users at the same time using spatially selective transmission [2]–[4]. Complementary to the urge for high throughputs under resource-limited communication systems, quality of service (QoS) is a vital requirement in modern communications. Designing the adaptive beamformers to optimize the QoS the for downlink channel has been extensively studied [4]–[10]. QoS is usually measured as a function of signal to interference plus noise ratio (SINR).

In addition to the above linear beamforming approaches, non-linear precoders such as Dirty paper coding (DPC) and Tomlinson-Harashima Precoding (THP) exploit the symbol information to pre-cancel potential interference at the transmitter [11]–[13]. Vector perturbation (VP) precoding presents a complementary approach that employs a non-linear symbol perturbation at the transmitter to further improve performance [14]–[19]. Nevertheless, both families of techniques involve non-linear designs, while VP in particular necessitates sophisticated search algorithms with a complexity that grows exponentially with the number of users [14], [15]. To reduce the complexity, several heuristic approaches have been studied [13], [20], [21]. However, none of the above are practical in current communication standards due to their high computational complexity. On the other hand, the zero-forcing (ZF) precoding [22], [23] is well known to have the least complexity amongst multi-user precoding approaches due to its closed form operation that involves an inversion of the channel matrix, but it performs far from the optimum in most scenarios. Accordingly, optimization-based downlink beamforming problems are considered. One approach is to minimize the total transmit power subject to the minimum SINR requirements at each user [5]. The uplink-downlink duality theory was established in [5] and [6]. Under the duality theorem, the downlink beamforming problem was efficiently solved using an iterative algorithm. In [6], an alternative downlink beamforming problem of maximizing the minimum SINR subject to a total power constraint was also developed and can be solved using the similar iterative algorithm. Conic optimization approaches to solving the downlink beamforming problem have also been explored [7]–[9]. Using semidefinite relaxation (SDR) technique [24], the rank-relaxed downlink beamforming problem becomes a convex optimization, which can be efficiently solved by contemporary linear or nonlinear programming methods such as the subgradient projection and barrier methods to obtain an optimal solution [25]. It is proved that a rank-one solution exists when the problem is feasible [7], [8]. In [26] and [27], the authors provided a rank-reduction algorithm to reduce the rank of the relaxed solution. For downlink beamforming with additional shaping constraints, it has been shown in [26] and [27] that if the number of additional shaping constraints is less than or equal to two, then rank-one solution can be obtained. A more advanced scheme was proposed in [28], which combines beamforming with high dimensional real-value orthogonal space time block coding (OSTBC) to increase the degrees of freedom in the optimization design. The authors in [9] formulated the problem into a second order cone program (SOCP) which allows the use of efficient solvers with reduced complexity. The channel robust worst-case downlink beamforming optimization designed to resist CSI errors was considered in [7] and [29]–[31]. As a

Manuscript received September 27, 2017; revised January 22, 2018 and April 4, 2018; accepted May 28, 2018. Date of publication June 7, 2018; date of current version November 16, 2018. This paper was presented in part at the IEEE International Conference on Acoustics Speech and Signal Processing, 2016 [1]. The associate editor coordinating the review of this paper and approving it for publication was X. Wang. *(Corresponding author: Christos Masouros.)*

The authors are with the Department of Electronic and Electrical Engineering, University College London, London WC1E 7JE, U.K. (e-mail: k.law@ucl.ac.uk; chris.masouros@ieee.org).

Color versions of one or more of the figures in this paper are available online at http://ieeexplore.ieee.org.

Digital Object Identifier 10.1109/TCOMM.2018.2843784

further step, outage probability (OP)-constrained downlink beamforming has been developed and it has been proved that both the worst channel robust and outage probabilistically constrained problems are equivalent [31], [32]. In particular, for a given radius of uncertainty set, one can obtain the OP such that both problems can be derived to the same formulation and vice versa.

In the SINR-based downlink problem, beamformers are designed to guarantee that the SINR constraints are satisfied. However, the disadvantage of the conventional SINR criteria that treat interference as harmful is that critical power is wasted by suppressing, eliminating and avoiding the interference. Making use of both the CSI and data information, rather than mitigating it, one can exploit the constructive part of interference to enhance the useful signal. The concept of interference exploitation was introduced in [20] and [33]–[43]. This is also referred to as a constructive interference precoding. In [20], [34]–[39], and [44], the closed-form linear and nonlinear precoders were discussed by exploiting the constructive interference to achieve higher SINRs without additional transmit power. Nevertheless, these precoders are not fully optimized. In more recent work, the authors in [16], [40], and [41] developed optimization-based precoders by designing beamforming which exploits constructive interference and can further reduce the transmit power. One particular optimization problem is to minimize the transmit power while guaranteeing certain signal to noise ratio (SNR) thresholds for all users and at the same time accommodate constructive interference to enhance the useful signal. This was first introduced in [16] as a linear adaptation of VP, and then applied to beamforming optimization. A conservative approach was offered in [41], by restricting the resultant interference to shift the received symbol in the exact same angle with the intended symbol, while a relaxed method was developed [40] A related transmitter-side precoding technique, namely directional modulation, exploits the constellation formats to achieve physical-layer security [45]–[47].

In line with the above, this paper is based on the downlink beamforming optimization by exploiting constructive interference to enhance the useful signal [40], [41], [48], [49]. In line with the above, we assume a TDD transmission, and the availability of CSI and instantaneous data at the transmitter. We investigate different quantitative measures of QoS as objective functions and optimize these subject to power constraints. While closed-form sum rate expressions do not apply to the modulation-dependent concept of interference exploitation [40], motivated by the error rate comparisons in the relevant literature [34]– [41], we focus on error rate related metrics detailed in the sequence. All proposed approaches can be formulated into convex optimizations. The contributions of this paper can be summarized as follows:

1) We propose a detection-region based downlink beamforming problem in Section IV by introducing a new geometrical analysis to the optimization problem studied in [40].
2) We reformulate the optimization to address the worst user EP downlink beamforming problem in Sections V and VI and show the detection-region based and EP-based problems exhibit a one to one correspondence in Section V.
3) We provide an analytic bound of average symbol error rate (SER) performance by solving the sum EPs optimization. It is observed in the simulations that the analytic SER results closely match with the experimental SER results.
4) Computationally-efficient solver algorithms are developed for each approach in Sections IV, V, and VI, respectively.

In the following analysis, we focus on phase-shift keying (PSK) modulation which offers notational simplicity in the definition of constructive interference. This is further motivated by the fact that the concept of interference exploitation is most useful in high-interference scenarios where low order modulation such as BPSK and QPSK is employed to ensure the reliability [50]. Nevertheless, our analysis and designs can be readily extended to other modulation schemes such as quadrature amplitude modulation (QAM) by trivially applying the approaches in [38] and [43], [51]–[54], which specifically treat the topic of interference exploitation for QAM transmission. Regarding the closest literature on interference exploitation in [40] we note that the contributions in our paper involve a) a noise robust downlink beamforming problem by introducing a geometrical analysis to the optimization problem studied in [40], b) a new formulation of the optimization to address the worst user error probability, c) derivation of a tight analytic bound of average SER performance where previously no such bounds existed, d) computationally-efficient solver algorithms developed for each of the proposed approaches.

The remainder of the paper is organized as follows. Section II introduces the signal model and revisits the conventional downlink beamforming problem. Section III outlines the constructive interference-based optimization. Section IV formulates the detection-region based downlink beamforming problem. Section V develops the worst user EP downlink beamforming problem. Section VI presents the sum EPs downlink beamforming problem. Simulation results are provided in Section VII and conclusions are drawn in Section VIII.

Notation: $\mathrm{E}(\cdot)$, $\Pr(\cdot)$, $|\cdot|$, $\|\cdot\|$, $(\cdot)^*$i¼Œ $(\cdot)^T$, denote statistical expectation, the probability, the absolute value, the Euclidean norm, the complex conjugate, and the transpose, respectively. $\mathbf{I}_j$, and $\mathbf{a}_j$ denotes the $j \times j$ identity matrix, $j \times 1$ vector of all a, respectively. $\mathrm{Re}(\cdot)$ and $\mathrm{Im}(\cdot)$ are the real part, and the imaginary part, respectively. $\lceil a \rceil$ is the smallest integer greater than or equal to a.

II. System Model and Conventional Downlink Beamforming

Consider a downlink scenario, where a single N-antenna BS transmits signals to K single-antenna users. Assume that the noise n_i at the ith user is circularly symmetric complex Gaussian with zero mean, i.e., $n_i \sim \mathcal{CN}(0, \sigma^2)$ where σ^2 is the noise variance. Let b_i and $\mathbf{h}_i$ be the unit amplitude of the M-order PSK (M-PSK) modulated symbol and $N \times 1$ channel vector for the ith user, respectively. The transmit signal at the

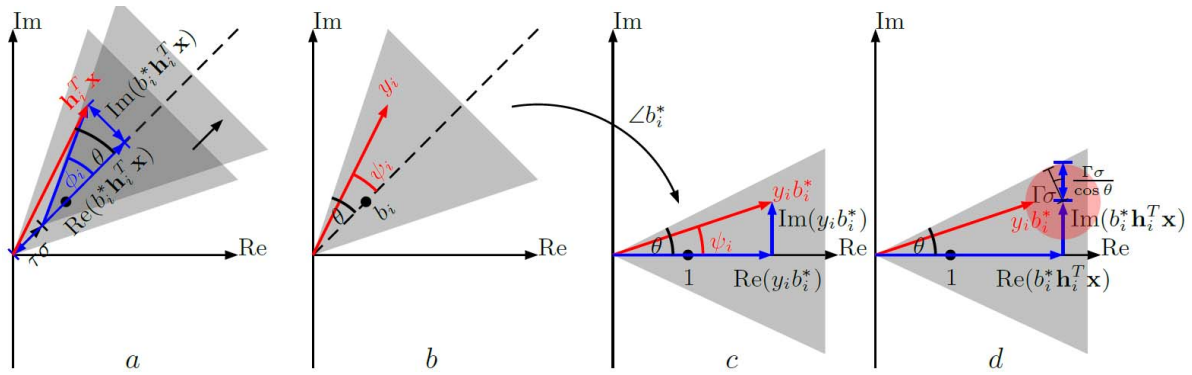

Fig. 1. In M-PSK, (a) precoding for interference exploitation and generic optimization [40] where the grey area is the constructive area of constellation; (b) constructive interference y_i within correct detection region; (c) after rotation by $\angle b_i^*$, $\mathrm{Re}(y_i b_i^*)$ and $\mathrm{Im}(y_i b_i^*)$ are projected from $y_i b_i^*$ on real and imaginary axis, respectively; (d) the detection region approach is described using trigonometry.

BS is the $N \times 1$ vector

$$\mathbf{x} = \sum_{i=1}^{K} \mathbf{t}_i b_i, \tag{1}$$

where $\mathbf{t}_i$ is the $N \times 1$ beamforming vector for the ith user. The signal received by the ith user is given by

$$\begin{aligned} y_i &= \mathbf{h}_i^T\mathbf{x} + n_i, \\ &= \underbrace{\mathbf{h}_i^T\mathbf{t}_i b_i}_{\text{desired signal}} + \underbrace{\sum_{j=1, j\neq i}^{K} \mathbf{h}_i^T\mathbf{t}_j b_j + n_i}_{\text{interference plus noise}}. \end{aligned} \tag{2}$$

The received SINR for the ith user is written as

$$\mathrm{SINR}_i \triangleq \frac{|\mathbf{h}_i^T\mathbf{t}_i|^2}{\sum_{\substack{j=1 \\ j\neq i}}^{K} |\mathbf{h}_i^T\mathbf{t}_j|^2 + \sigma^2}. \tag{3}$$

The mean total transmit power P_T over transmit symbols is defined as

$$P_T \triangleq \mathrm{E}\{\|\sum_{i=1}^{K} \mathbf{t}_i b_i\|^2\} = \sum_{i=1}^{K} \|\mathbf{t}_i\|^2. \tag{4}$$

We note that while above we consider a single carrier system model for notational simplicity in line with our benchmarks [6], [40], our approach can readily be extended to a MIMO-OFDM transmission where the involved precoding optimization can be applied on a per subcarrier basis. Below we present the two most common downlink beamforming optimization problems in the literature [5]–[8].

A. SINR Balancing

Our first benchmark optimization involves maximizing the minimum SINR subject to a predefined total transmit power. The problem can be written as [6]

$$\begin{aligned} \max_{\mathbf{t}_i, \gamma} \gamma \quad \text{s.t.} \quad & \frac{|\mathbf{h}_i^T\mathbf{t}_i|^2}{\sum_{\substack{j=1 \\ j\neq i}}^{K} |\mathbf{h}_i^T\mathbf{t}_j|^2 + \sigma^2} \geq \gamma, \quad \forall i = 1, \ldots, K, \\ & \sum_{i=1}^{K} \|\mathbf{t}_i\|^2 \leq P_0, \end{aligned} \tag{5}$$

where P_0 is the predefined total transmit power threshold.

B. Power Minimization

A relevant approach aims to minimize the total transmit power under the SINR constraints, in the form [6]

$$\begin{aligned} \min_{\mathbf{t}_i} \quad & \sum_{i=1}^{K} \|\mathbf{t}_i\|^2 \\ \text{s.t.} \quad & \frac{|\mathbf{h}_i^T\mathbf{t}_i|^2}{\sum_{\substack{j=1 \\ j\neq i}}^{K} |\mathbf{h}_i^T\mathbf{t}_j|^2 + \sigma^2} \geq \gamma_0, \forall i = 1, \ldots, K, \end{aligned} \tag{6}$$

where γ_0 is the minimal acceptable SINR. However, these problems do not consider the data symbols as a part of the optimization problem for each transmission. In this paper, we aim to design the downlink beamforming problem where we take the given symbols into account, to exploit constructive interference.

III. Constructive Interference Optimization-Based Precoding

Interference is a major limitation in wireless networks. In conventional downlink beamforming [6], a critical part of the transmit power is wasted to suppress the interference. It has recently been shown that, by exploiting the instantaneous interference, the received signals can be pushed further into the correct detection region, which improves the system performance [34], [35]. With the knowledge of the CSI and user data available at the transmitter, the constructive interference optimization precoder given in [40] improves upon the above optimizations to design beamformers to maximize the distance $\Gamma\sigma$ between the desired detection region in Fig. 1(a) that the received symbols must fall into, and the decision thresholds of the corresponding constellation point. This is done such that the resultant received symbol $\mathbf{h}_i^T\mathbf{x}$ falls within the corresponding constructive area of constellation, as shown in Fig. 1(a). That is, the area in the symbol constellation where the distances to the decision thresholds are increased with respect to the constellation point of interest. The design moves the resultant received symbol away from the original decision thresholds of the constellation, which improves the QoS. To avoid extensive repetition, the reader is referred to [40]

for the details of the underlying concept. Here, we recapture the optimization problem in the mathematical form as [40]

$$\max_{\mathbf{x},\Gamma} \ \Gamma$$
$$\text{s.t. } |\phi_i(\mathbf{x},\Gamma)| \le \theta, \tag{7a}$$
$$\|\mathbf{x}\|^2 \le P_0, \quad \forall i = 1,\ldots,K, \tag{7b}$$

where Γ is a scalar auxiliary variable that is equivalent to the minimum distance in the constellation region that will become clear in the following, $\theta = \pi/M$ and P_0 is the total transmit power threshold. The constraints in (7a) come from the fact that the resultant received symbol for the ith user lays on the constructive area of the constellation, if and only if

$$-\theta \le \phi_i \le \theta \tag{8}$$

where ϕ_i in Fig. 1(a) is the angle such that

$$\phi_i(\mathbf{x},\Gamma) = \begin{cases} \tan^{-1}\Big(\dfrac{\mathrm{Im}(b_i^*\mathbf{h}_i^T\mathbf{x})}{\mathrm{Re}(b_i^*\mathbf{h}_i^T\mathbf{x}) - \Gamma\sigma}\Big) & \mathrm{Re}(b_i^*\mathbf{h}_i^T\mathbf{x}) > \Gamma\sigma, \\ 0 & b_i^*\mathbf{h}_i^T\mathbf{x} = \Gamma\sigma. \end{cases} \tag{9}$$

and the physical meaning of $\Gamma\sigma$ in (9) is the distance of the correct detection region in Fig. 1(a) away from origin along with the direction of the corresponding constellation point. By substituting (9) into (7) and taking both sides by $\tan$, the problem (7) can be equivalently written as

$$\max_{\mathbf{x},\Gamma} \Gamma \ \ \text{s.t. } |\mathrm{Im}(b_i^*\mathbf{h}_i^T\mathbf{x})| \le (\mathrm{Re}(b_i^*\mathbf{h}_i^T\mathbf{x}) - \Gamma\sigma)\tan\theta,$$
$$\|\mathbf{x}\|^2 \le P_0, \quad \forall i = 1,\ldots,K. \tag{10}$$

The corresponding power minimization is written as [40]

$$\min_{\mathbf{x}} \|\mathbf{x}\|^2 \ \ \text{s.t. } |\mathrm{Im}(b_i^*\mathbf{h}_i^T\mathbf{x})| \le (\mathrm{Re}(b_i^*\mathbf{h}_i^T\mathbf{x}) - \Gamma_0\sigma)\tan\theta,$$
$$\forall i = 1,\ldots,K, \tag{11}$$

where $\Gamma_0\sigma$ is the minimal acceptable distance of the correct detection region. We note that (10),(11) correspond to the conventional SINR balancing and Power minimization problems (5),(6) where the SINR objsectives/constraints have been reformulated to accommodate constructive interference.

From Fig. 1(a), we can see the real projection of the resultant symbol is parallel to the signal and imaginary projection of the resultant symbol is perpendicular to the signal. Therefore, the approach in [40] treats Γ as an SNR-related variable, where it is shown that the SNR can defined as the instantaneous power of the real projection of the resultant symbol over the expectation of noise power, i.e., $\Gamma^2 = \frac{\min_{i=1}^K\{\mathrm{Re}(b_i^*\mathbf{h}_i^T\mathbf{x}_{CI}^\star)^2\}}{\sigma^2}$ where $\mathbf{x}_{CI}^\star$ is an optimal solution of transmit signal in (10). In the following section, instead of using the SNR as a measure of QoS, we introduce a detection-region based adaptation of the above constructive interference-based beamformers.

IV. Detection-Region Based Beamforming Optimization

In this section, we improve upon optimizations (10) and (11) by introducing a detection-region based adaptation. First we introduce an alternative systematic treatment of constructive interference as per Fig. 1. For PSK modulation, interference is constructive if the received signal y_i falls within the correct detection region, which is the shaded area shown in Fig. 1(b). It is important to note that, here we consider the resultant received symbol y_i including noise is considered, whereas the resultant received symbol $\mathbf{h}_i^T\mathbf{x}$ excluding is discussed in [40]. Accordingly, we are interested in the constraints that the received symbol y_i falls inside the correct detection region in the constellation, given a certain noise variance. Under this new definition, we have the following lemma.

Lemma 1: The received signal y_i benefits from constructive interference, if and only if

$$-\theta \le \psi_i \le \theta \tag{12}$$

where ψ_i in Fig. 1(b) is the angle between the received signal y_i and the transmit symbol b_i and is also treated as a function in terms of $\mathbf{x}$ and n_i such that

$$\psi_i(\mathbf{x}, n_i) = \begin{cases} \tan^{-1}\big(\dfrac{\mathrm{Im}(y_i b_i^*)}{\mathrm{Re}(y_i b_i^*)}\big) & \mathrm{Re}(y_i b_i^*) > 0, \\ 0 & y_i b_i^* = 0. \end{cases} \tag{13}$$

Proof: To find out the angle ψ_i that ensures constructive interference, we first rotate Fig. 1(b) to Fig. 1(c) by shifting the constellation by a phase equal to $-\angle b_i$, i.e., by multiplying b_i^*. Since b_i has unit power, $y_i b_i^*$ does not change the magnitude of the complex number. Then we obtain (13) where $\mathrm{Im}(y_i b_i^*)$ and $\mathrm{Re}(y_i b_i^*)$ are the projection of $y_i b_i^*$ onto the real and imaginary axis, respectively. ∎

Based on the above, the classification criterion (12) can be reformulated as the following constraints

$$\frac{|\mathrm{Im}(y_i b_i^*)|}{\mathrm{Re}(y_i b_i^*)} \le \tan\theta, \tag{14}$$
$$\mathrm{Re}(y_i b_i^*) > 0, \tag{15}$$

which is equivalent to the following single constraint

$$|\mathrm{Im}(y_i b_i^*)| - \mathrm{Re}(y_i b_i^*)\tan\theta \le 0. \tag{16}$$

A. Noise Uncertainty Radius Maximization

As shown in Fig. 1(d), for a given received signal excluding noise (denoted by the red arrow in the figure) one has to apply the noise uncertainty region such that the received symbols including noise obey the required SNR Γ with respect to the detection thresholds of the modulation constellation, denoted by the bounds of the grey region in the figure. The idea of the detection-region based downlink beamforming problem is to design the beamforming weight vector and the radius $\Gamma\sigma$ of the noise uncertainty set such that if the noise is within the noise uncertainty set, then it guarantees that the given received signal falls into the constructive area of the constellation and can be decoded without any error, i.e., y_i benefits from constructive interference. Given the noise variance σ^2, the optimization aims to maximize the radius $\Gamma\sigma$ of the noise uncertainty set such that it can still satisfy the constraints (16) under the

power budget. The resulting detection-region based downlink beamforming problem can be expressed as

$$\max_{\mathbf{x},\Gamma} \Gamma \tag{17}$$

$$\text{s.t.} \max_{\|n_i\|\le\Gamma\sigma} |\psi_i(\mathbf{x},n_i)| \le \theta, \quad \forall i=1,\ldots,K,$$
$$\|\mathbf{x}\|^2 \le P, \tag{18}$$

where P is the maximum allowable total transmit power. By Lemma 1 and (16), problem (18) can be rewritten as

$$\max_{\mathbf{x},\Gamma} \ \Gamma$$

$$\text{s.t.} \max_{\|n_i\|\le\Gamma\sigma} |\operatorname{Im}(y_i b_i^*)| - \operatorname{Re}(y_i b_i^*)\tan\theta \le 0, \tag{19a}$$
$$\|\mathbf{x}\|^2 \le P, \ \forall i=1,\ldots,K. \tag{19b}$$

We can first solve the inner maximization on the left side of (19a).

Corollary 1: For a fixed $\tilde{\mathbf{x}}$, the optimal solution of the inner maximization in (19) is given by

$$|\operatorname{Im}(b_i^*\mathbf{h}_i^T\tilde{\mathbf{x}})| + \Gamma\sigma/\cos\theta - \operatorname{Re}(b_i^*\mathbf{h}_i^T\tilde{\mathbf{x}})\tan\theta. \tag{20}$$

Proof: See Appendix A. ∎

According to Corollary 1, problem (19) can be rewritten as a function $\Gamma^\star(\cdot)$ for any given $P \ge 0$ such that

$$\Gamma^\star(P): \max_{\mathbf{x},\Gamma} \ \Gamma$$
$$\text{s.t.} \ |\operatorname{Im}(b_i^*\mathbf{h}_i^T\mathbf{x})| + \Gamma\sigma/\cos\theta \le \operatorname{Re}(b_i^*\mathbf{h}_i^T\mathbf{x})\tan\theta,$$
$$\|\mathbf{x}\|^2 \le P, \quad \forall i=1,\ldots,K. \tag{21}$$

The problem in (21) can be solved using available convex optimization tools [55]. Finally, we can set the optimal beamforming vector $\mathbf{t}_i^\star$ in (1) as

$$\mathbf{t}_i^\star = \frac{\mathbf{x}^\star b_i^*}{K}, \tag{22}$$

where $\mathbf{x}^\star$ is an optimal solution of transmit signal in (21). Note that (10) and (21) are only different by a constant. Suppose $\mathbf{x}_{SD}^\star$ and $\mathbf{x}_{NR}^\star$ are optimal solutions of transmit signal in (10) and (21), respectively. Then $\sin\theta\mathbf{x}_{NR}^\star = \mathbf{x}_{SD}^\star$. Therefore we can treat them as equivalent problems.

B. Trigonometrical Equivalence

The optimization problem (21) can also be explained using trigonometry. The Fig. 1(d) uses a trigonometrical approach by maximizing the radius $\Gamma\sigma$ of the noise uncertainty set within the shaded region. As seen in the figure, $\Gamma\sigma/\cos\theta$ is the projection of $\Gamma\sigma$ on the imaginary axis. By observing the trigonometry in Fig. 1(d), we have

$$\frac{|\operatorname{Im}(b_i^*\mathbf{h}_i^T\mathbf{x})| + \Gamma\sigma/\cos\theta}{\operatorname{Re}(b_i^*\mathbf{h}_i^T\mathbf{x})} \le \tan\theta, \tag{23}$$

$$\operatorname{Re}(b_i^*\mathbf{h}_i^T\mathbf{x}) > 0, \tag{24}$$

or

$$b_i^*\mathbf{h}_i^T\mathbf{x} = 0, \tag{25}$$

$$\Gamma = 0, \tag{26}$$

which is equivalent to

$$|\operatorname{Im}(b_i^*\mathbf{h}_i^T\mathbf{x})| + \Gamma\sigma/\cos\theta \le \operatorname{Re}(b_i^*\mathbf{h}_i^T\mathbf{x})\tan\theta. \tag{27}$$

which yields directly (21).

C. The Power Minimization Problem

In this subsection, we present the power minimization that is related to (21), and employ this formulation to design an efficient solver. The downlink beamforming optimization is to minimize the total transmit power such that noise in the given uncertainty set falls within the constructive area of the constellation. Based on (21) the problem can be written as

$$\min_{\mathbf{x}} \|\mathbf{x}\|^2 \ \text{ s.t.} \max_{\|n_i\|\le\Gamma\sigma} |\psi_i(\mathbf{x},n_i)| \le \theta, \quad \forall i=1,\ldots,K. \tag{28}$$

Using a similar approach as in Subsection IV-A, we can reformulate problem (28) as a function $P^\star(\cdot)$ for any given $\Gamma \ge 0$ such that

$$P^\star(\Gamma): \min_{\mathbf{x}} \ \|\mathbf{x}\|^2$$
$$\text{s.t.} \ |\operatorname{Im}(b_i^*\mathbf{h}_i^T\mathbf{x})| + \Gamma\sigma/\cos\theta \le \operatorname{Re}(b_i^*\mathbf{h}_i^T\mathbf{x})\tan\theta,$$
$$\forall i=1,\ldots,K. \tag{29}$$

Similarly, we notice that (11) and (29) can be treated as equivalent problems. To obtain a real-valued representation of the optimization that allows efficient solvers following [40], let us denote

$$\bar{\mathbf{x}} \triangleq [\operatorname{Re}(\mathbf{x})^T \ \operatorname{Im}(\mathbf{x})^T]^T, \tag{30}$$

$$\bar{\mathbf{h}}_i \triangleq [\operatorname{Im}(b_i^*\mathbf{h}_i)^T \ \operatorname{Re}(b_i^*\mathbf{h}_i)^T]^T, \tag{31}$$

$$\mathbf{\Pi}_K \triangleq [\mathbf{0}_{K,K} \ -\mathbf{I}_K; \mathbf{I}_K \ \mathbf{0}_{K,K}], \tag{32}$$

where $\mathbf{0}_{K,K}$ is the $K\times K$ zero matrix. Then we can express the real part and imaginary part in (29) as follows

$$\operatorname{Re}(b_i^*\mathbf{h}_i^T\mathbf{x}) = \bar{\mathbf{h}}_i^T\mathbf{\Pi}_K\bar{\mathbf{x}}, \tag{33}$$

$$\operatorname{Im}(b_i^*\mathbf{h}_i^T\mathbf{x}) = \bar{\mathbf{h}}_i^T\bar{\mathbf{x}}. \tag{34}$$

Using (30), (33) and (34), we can rewrite (29) as

$$\min_{\bar{\mathbf{x}}} \ \|\bar{\mathbf{x}}\|^2 \ \text{ s.t.} \ -\mathbf{T}\bar{\mathbf{x}} + \Gamma\mathbf{1}_{2K} \le \mathbf{0}_{2K}, \tag{35}$$

where $\mathbf{T}$ is a $2K\times 2N$ matrix such that

$$\mathbf{T} \triangleq \frac{\cos\theta}{\sigma}\begin{pmatrix} -\bar{\mathbf{h}}_1^T + \tan\theta\bar{\mathbf{h}}_1^T\mathbf{\Pi}_K \\ \bar{\mathbf{h}}_1^T + \tan\theta\bar{\mathbf{h}}_1^T\mathbf{\Pi}_K \\ \vdots \\ -\bar{\mathbf{h}}_K^T + \tan\theta\bar{\mathbf{h}}_K^T\mathbf{\Pi}_K \\ \bar{\mathbf{h}}_K^T + \tan\theta\bar{\mathbf{h}}_K^T\mathbf{\Pi}_K \end{pmatrix}. \tag{36}$$

The Lagrangian associated with (35) is given by

$$L(\bar{\mathbf{x}},\mathbf{u}) = \|\bar{\mathbf{x}}\|^2 + \mathbf{u}^T(-\mathbf{T}\bar{\mathbf{x}} + \Gamma\mathbf{1}_{2K}), \tag{37}$$

where $\mathbf{u}$ is a $2K\times 1$ vector. Setting $\partial L(\bar{\mathbf{x}},\mathbf{u})/\partial\bar{\mathbf{x}} = \mathbf{0}_{2K}$, we obtain

$$\bar{\mathbf{x}}^\star = \frac{1}{2}\mathbf{T}^T\mathbf{u}^\star. \tag{38}$$

Substituting (36) into (37), we write the dual problem of (35) as

$$\max_{\mathbf{u}\geq\mathbf{0}_{2K}} \; -\frac{\|\mathbf{T}^T\mathbf{u}\|^2}{4}+\Gamma\mathbf{1}_{2K}^T\mathbf{u}, \tag{39}$$

which is equivalent to

$$-\min_{\mathbf{u}\geq\mathbf{0}_{2K}} \; f(\mathbf{u})\triangleq\frac{\|\mathbf{T}^T\mathbf{u}\|^2}{4}-\Gamma\mathbf{1}_{2K}^T\mathbf{u}. \tag{40}$$

The above optimization can be solved effieicntly using the gradient descent algorithm with simple bound constraints [56]. The gradient of $f(\mathbf{u})$ is given by

$$\bigtriangledown\mathbf{f}(\mathbf{u})=\frac{\mathbf{T}\mathbf{T}^T\mathbf{u}}{2}-\Gamma\mathbf{1}_{2K}. \tag{41}$$

By substituting (38) into (35), problem (35) can be reformulated as

$$\min_{\mathbf{u}\geq\mathbf{0}_{2K}} \|\frac{1}{2}\mathbf{T}^T\mathbf{u}\|^2 \;\; \text{s.t.} \;\; -\bigtriangledown\mathbf{f}(\mathbf{u})\leq\mathbf{0}_{2K}. \tag{42}$$

Therefore, we need to guarantee at the optimal dual solution $\mathbf{u}^\star$ of problem (40) that

$$\bigtriangledown\mathbf{f}(\mathbf{u}^\star)\geq\mathbf{0}_{2K}. \tag{43}$$

If the condition of (43) is violated, then either the gradient descent algorithm has a low convergence rate or (42) is infeasible. The feasibility of (42) can be examined by solving the following problem:

$$\text{find } \mathbf{u} \;\; \text{s.t.} -\bigtriangledown\mathbf{f}(\mathbf{u})\leq\mathbf{0}_{2K},\; \mathbf{u}\geq\mathbf{0}_{2K}. \tag{44}$$

which is a linear programming problem.

Algorithm 1 outlines the gradient descent method to solve (29) where $i_{\max}$ and Δ_t are the given maximum number of iterations and error tolerance, respectively. According to [57], the gradient descent method requires at most $\mathcal{O}(\Delta_t^{-2})$ iterations for $\Delta_t>0$ arbitrarily small. However, it is an open question whether the above bound is tight or not. For the ill-conditioned problems, the convergence rate of gradient descent may be poor. It is important to note at this point that that computational complexity is key for all interference exploitation approaches. Indeed, while conventional beamforming needs to be optimized whenever the channel changes, interference exploitation optimizations are data-dependent, and need to be performed on a symbol-by-symbol basis. Accordingly, efficient solvers for reducing the complexity of obtaining the beamformers are indispensable, and we derive a number of efficient approaches in the following.

Algorithm 1 Gradient Descent Algorithm to Solve (29)

Input: $\{\mathbf{h}_i\}_{i=1}^K,\{b_i\}_{i=1}^K,\Gamma_0,\sigma$
Output: The optimal solution $\bar{\mathbf{x}}^\star$ of problem (29)
Initialize randomly $\mathbf{u}^{(0)}$ and $i=0$;
repeat
  $i=i+1$;
  if $i>i_{\max}$ **then**
    Exit and output no solution;
  end if
  Compute the gradient descent direction $\bigtriangledown\mathbf{f}(\mathbf{u}^{(i-1)})$;
  Choose a_i via backtracking linear search;
  $\mathbf{u}^{(i)}=\max\Big(\mathbf{0}_{2K},\mathbf{u}^{(i-1)}-a_i\bigtriangledown\mathbf{f}(\mathbf{u}^{(i-1)})\Big)$;
until $\|\mathbf{u}^{(i)}-\mathbf{u}^{(i-1)}\|<\Delta_t$ and $\min\bigtriangledown\mathbf{f}(\mathbf{u}^{(i)})>-\Delta_t$;
Output $\bar{\mathbf{x}}^\star=\mathbf{T}^T\mathbf{u}^{(i)}/2$;

D. An Efficient Algorithm for Power Minimization of (29) Based on the Barrier Method

It will be shown in the simulation results that Algorithm 1 can have a low convergence rate. In this subsection, we propose the barrier method as an alternative to compute the optimal solution of the power minimization in (29). Let

$$\phi(\mathbf{u})=-\mathbf{1}_{2K}^T\ln(\mathbf{u}) \tag{45}$$

be the logarithmic barrier function where natural logarithm $\ln(\cdot)$ is an elementwise operator. We note that the barrier method based on the logarithmic barrier function, as above, is identical to the primal-dual interior point method [54]. For $s>0$, define $\mathbf{u}^\star(s)$ as the solution of

$$\min_{\mathbf{u}} \;\; sf(\mathbf{u})+\phi(\mathbf{u}). \tag{46}$$

Problem (46) can be solved using the gradient descent algorithm. It has been shown in [25] that the number of gradient descent iterations is of the order $\mathcal{O}(\frac{\log(K/\Delta_t)}{\log\mu})$ for the barrier method. In general, the barrier method is a more practical approach to solve a convex optimization problem as it provides a guarantee on the convergence rate compared to the gradient descent method. The algorithm to efficiently solve (29) is shown in Algorithm 2. It will be shown in the simulations that this provides much faster convergence than Algorithm 1.

Algorithm 2 Efficient Barrier Method Algorithm to Solve (29)

Input: $\{\mathbf{h}_i\}_{i=1}^K,\{b_i\}_{i=1}^K,\Gamma_0,\sigma,\mu$
Output: The optimal solution of transmit signal $\bar{\mathbf{x}}^\star$ in problem (29)
if (44) has no solution **then**
  Exit and output infeasible;
else
  Set $\mathbf{u}^\star(1)$ to be the solution of (44);
end if
repeat
  Compute $\mathbf{u}^\star(s)$ of (46) ;
  Set $s=\mu s$;
until $\|\mathbf{u}^\star(s)-\mathbf{u}^\star(s-1)\|<\Delta_t$ and $\min\bigtriangledown\mathbf{f}(\mathbf{u}^\star(s))>-\Delta_t$;
Output $\bar{\mathbf{x}}^\star=\mathbf{T}^T\mathbf{u}^\star(s)/2$;

E. An Efficient Detection-Region Based Algorithm

Based on the above formulation, in this subsection we refocus our attention to problem (21) and provide an efficient algorithm for solving the detection-region based beamforming problem. First of all, we show that the solution of (21) can be obtained by solving (29). Then based on this fact, we present an efficient algorithm to solve (21).

Let $\mathbf{x} = \sqrt{P}\check{\mathbf{x}}$ such that $\|\check{\mathbf{x}}\|^2 = 1$. Then problem (21) can be rewritten as

$$\begin{aligned} &\max_{\check{\mathbf{x}},\Gamma} \ \Gamma \\ &\text{s.t. } |\operatorname{Im}(b_i^* \mathbf{h}_i^T \check{\mathbf{x}})| + \frac{\Gamma\sigma}{\sqrt{P}\cos\theta} \le \operatorname{Re}(b_i^* \mathbf{h}_i^T \check{\mathbf{x}}) \tan\theta, \\ &\quad \|\check{\mathbf{x}}\|^2 \le 1, \quad \forall i = 1, \ldots, K. \end{aligned} \tag{47}$$

Problem (47) implies that Γ is directly proportional to $\sqrt{P}$. Hence, we have the following relations:

$$\Gamma^\star(P) = \sqrt{P}\Gamma^\star(1), \tag{48}$$

$$\mathbf{x}_\Gamma^\star(P) = \sqrt{P}\mathbf{x}_\Gamma^\star(1), \tag{49}$$

where $\mathbf{x}_\Gamma^\star(\tilde{P})$ is an optimal solution of transmit signal in (21) for a given total transmit power $\tilde{P}$. Similarly, if $P^\star(1)$ is feasible, then we have the following relations:

$$P^\star(\Gamma) = \Gamma^2 P^\star(1), \tag{50}$$

$$\mathbf{x}_P^\star(\Gamma) = \Gamma \mathbf{x}_P^\star(1), \tag{51}$$

where $\mathbf{x}_P^\star(\tilde{\Gamma})$ is an optimal solution of transmit signal in (29) for a given noise uncertainty set radius $\tilde{\Gamma}\sigma$.

Remark: Problem (21) is always feasible for any given power P_0 as the trivial solution is one of the candidate solutions. Suppose $\Gamma^\star(1) \neq 0$. Then, using a similar argument as in [6] we have that

$$\|\mathbf{x}_\Gamma^\star(P)\|^2 = P. \tag{52}$$

The following two Corollaries show the we can obtain the solution of (21) by solving (29) and vice versa.

Corollary 2: Let $\Gamma_0\sigma$ and P_0 be the given positive noise uncertainty set radius and total transmit power. Suppose $P^\star(1)$ is feasible. Then we obtain

$$\Gamma^\star(P^\star(\Gamma_0)) = \Gamma_0, \tag{53}$$

$$\mathbf{x}_\Gamma^\star(P^\star(\Gamma_0)) = \mathbf{x}_P^\star(\Gamma_0). \tag{54}$$

Conversely, suppose $\Gamma^\star(1) \neq 0$. Then we can also obtain

$$P^\star(\Gamma^\star(P_0)) = P_0, \tag{55}$$

$$\mathbf{x}_P^\star(\Gamma^\star(P_0)) = \mathbf{x}_\Gamma^\star(P_0). \tag{56}$$

Proof: See Appendix B. ∎

Corollary 3: Suppose $\Gamma^\star(1) \neq 0$. Then problem (29) always has non-trivial solution for any given Γ_0.

Proof: See Appendix C. ∎

According to Corollary 2 and Corollary 3, once the optimal solution of (29) is known, which can be efficiently found through Algorithms 1-2, the solution to (21) can be found in closed form. Accordingly, we can derive an efficient algorithm for solving (21) using Algorithm 2. Algorithm 3 below presents the algorithm used to compute the optimal solution of (21).

Algorithm 3 Algorithm to Solve (21)

Input: $\{\mathbf{h}_i\}_{i=1}^K, \{b_i\}_{i=1}^K, P_0, \sigma$
Output: The solution $\mathbf{x}^\star$ of problem (21)
$(P^\star(1), \mathbf{x}_P^\star(1))$ be the solution of (29) by Algorithm 2;
if $P^\star(1)$ is feasible and it is not a trivial solution **then**
  Set $\tilde{\Gamma} = \sqrt{P_0/P^\star(1)}$;
  $(\tilde{\Gamma}\mathbf{x}_P^\star(1), \tilde{\Gamma})$ be the optimal solution of (21);
else
  Output the trivial solution: $\tilde{\Gamma} = 0, \mathbf{x}_P^\star = \mathbf{0}_K$;
end if

V. Worst User Error Probability Approach

In this section, we propose a new approach to downlink beamforming based on the error probability. The main concept is to replace the detection-region based downlink beamforming constraints by more flexible probabilistic constraints. We define the EP for ith user as the probability that the received signals of ith user fall inside the left or right half plane of Fig. 1(b), i.e., regions bounded between θ and $\pi + \theta$ or between $-\theta$ and $-\pi - \theta$, respectively, for which case incorrect detection occurs. The EP optimization problem for the worst user minimizes the maximum EP and can be written as

$$\begin{aligned} &\min_{\mathbf{x},p} \ p \\ &\text{s.t. } \Pr\Big(\pi + \theta \ge \psi_i(\mathbf{x}, n_i) \ge \theta\Big) \le p, \quad \forall i = 1, \ldots, K, \end{aligned} \tag{57a}$$

$$\Pr\Big(-\pi - \theta \ge \psi_i(\mathbf{x}, n_i) \ge -\theta\Big) \le p, \quad \forall i = 1, \ldots, K,$$

$$\|\mathbf{x}\|^2 \le P. \tag{57b}$$

Remark: Problem (57) is different from the channel outage probability based downlink beamforming problem in [31] and [32]. The constraints in [31] and [32] are probabilistic SINR-based with respect to the *channel* random variables, while the constraints in our constructive interference-based optimization are adapted to reflect the EP due to *noise* random variables, in which the received signal falls outside the desired region of the constellation, in order to have a reliable detection. According to Lemma 1 and (16), problem (57) reduces to

$$\begin{aligned} &\min_{\mathbf{x},p} \ p \\ &\text{s.t. } \Pr\Big(\operatorname{Im}(y_i b_i^*) \ge \operatorname{Re}(y_i b_i^*) \tan\theta\Big) \le p, \end{aligned} \tag{58a}$$

$$\Pr\Big(\operatorname{Im}(y_i b_i^*) \le -\operatorname{Re}(y_i b_i^*) \tan\theta\Big) \le p,$$

$$\|\mathbf{x}\|^2 \le P, \forall i = 1, \ldots, K. \tag{58b}$$

Let

$$z_j = (-1)^{(j+1)} \operatorname{Im}(b_i^* \mathbf{h}_i^T \mathbf{x}) - \operatorname{Re}(b_i^* \mathbf{h}_i^T \mathbf{x}) \tan\theta, \tag{59}$$

$$\tilde{n}_j = (-1)^{(j+1)} \operatorname{Im}(b_i^* n_i) - \operatorname{Re}(b_i^* n_i) \tan\theta, \tag{60}$$

for $i = \lceil j/2 \rceil$ and $j = 1, \ldots, 2K$. The constraints in (58a) and (58b) can be reformulated as

$$\Pr(z_j + \tilde{n}_j \ge 0) \le p, \forall j = 1, ..., 2K. \tag{61}$$

Since n_i is a circularly symmetric complex Gaussian random variable, we get

$$\begin{aligned} \mathrm{E}\{\operatorname{Re}(b_i^* n_i)^2\} &= \mathrm{E}\{\operatorname{Im}(b_i^* n_i)^2\} \\ &= b_{Ri}^2 \frac{\sigma^2}{2} + b_{Ii}^2 \frac{\sigma^2}{2} = \frac{\sigma^2}{2}, \end{aligned} \tag{62}$$

$$\mathrm{E}\{\operatorname{Re}(b_i^* n_i) \operatorname{Im}(b_i^* n_i)\} = b_{Ri} b_{Ii} - b_{Ri} b_{Ii} = 0. \tag{63}$$

Then $\tilde{n}_j$ is a real-valued Gaussian random variable with zero mean such that

$$\mathrm{E}\{\tilde{n}_j^2\} = \frac{(1+\tan^2\theta)\sigma^2}{2} = \frac{\sigma^2}{2\cos^2\theta}, \tag{64}$$

i.e., $\tilde{n}_j \sim \mathcal{N}(0, \frac{\sigma^2}{2\cos\theta^2})$. Thus we have [32]

$$\Pr(z_j + \tilde{n}_j \geq 0) = \int_{-z_j}^{\infty} \frac{\cos\theta}{\sqrt{\pi}\sigma} e^{\frac{\tilde{n}^2\cos^2\theta}{\sigma^2}} d\tilde{n}.$$

Using the Gaussian error function $\mathrm{erf}(\cdot)$, we can write

$$\Pr(z_j + \tilde{n}_j \geq 0) = \begin{cases} \frac{1}{2} + \frac{1}{2}\mathrm{erf}\Big(\frac{z_j\cos\theta}{\sigma}\Big), & -z_j \leq 0, \\ \frac{1}{2} - \frac{1}{2}\mathrm{erf}\Big(\frac{-z_j\cos\theta}{\sigma}\Big), & -z_j \geq 0. \end{cases} \tag{65}$$

Since $\mathrm{erf}(-x) = -\mathrm{erf}(x)$, we rewrite it as

$$\frac{1}{2} - \frac{1}{2}\mathrm{erf}\Big(\frac{-z_j\cos\theta}{\sigma}\Big) \leq p, \tag{66}$$

which is equivalent to

$$|\,\mathrm{Im}(b_i^*\mathbf{h}_i^T\mathbf{x})| + \frac{\mathrm{erf}^{-1}(1-2p)\sigma}{\cos\theta} \leq \mathrm{Re}(b_i^*\mathbf{h}_i^T\mathbf{x})\tan\theta, \quad \forall i. \tag{67}$$

Thus, the worst user EP problem (58) can be written as

$$\begin{aligned} &\min_{\mathbf{x},p}\ p \\ &\text{s.t. } |\,\mathrm{Im}(b_i^*\mathbf{h}_i^T\mathbf{x})| + \frac{\mathrm{erf}^{-1}(1-2p)\sigma}{\cos\theta} \leq \mathrm{Re}(b_i^*\mathbf{h}_i^T\mathbf{x})\tan\theta, \\ &\quad \|\mathbf{x}\|^2 \leq P, \quad \forall i = 1,\ldots,K. \end{aligned} \tag{68}$$

Remark: By observation of (21) and (68) it can be seen that the optimal values of the two problems have the following relations:

$$\Gamma^\star(P) = \mathrm{erf}^{-1}(1-2\,p^\star(P)), \tag{69}$$

$$p^\star(P) = \frac{1}{2} - \frac{1}{2}\mathrm{erf}(\Gamma^\star(P)), \tag{70}$$

$$\mathbf{x}_p^\star(P) = \mathbf{x}_\Gamma^\star(P), \tag{71}$$

where $(\mathbf{x}_p^\star(\tilde{P}), p^\star(\tilde{P}))$ is an optimal solution of (68) for a given power $\tilde{P}$. The above relations show that given a radius of noise uncertainty set of (21), one can obtain the worst user EP of (68). In reverse, given an EP of (68), we can also obtain the radius of noise uncertainty set of (21). Therefore, we can treat the detection-region based problem (21) and the worst user EP-based problem (68) as equivalent problems. Using (49), we can express the worst user EP in terms of the total transmit power P as

$$p^\star(P) = \frac{1}{2} - \frac{1}{2}\mathrm{erf}\big(\sqrt{P}\Gamma^\star(1)\big), \tag{72}$$

$$\mathbf{x}_p^\star(P) = \sqrt{P}\mathbf{x}_\Gamma^\star(1). \tag{73}$$

VI. Sum EPs Approach

In this section, we build upon the EP optimization above to derive the sum EPs-based downlink beamforming problem. The important benefit here is that the sum EPs approach facilitates the derivation of an analytical bound, which is shown to be tight in our results section. Accordingly, we replace the EP for the worst user in (57), by the sum of the EPs for all users, in which the optimization problem provides an analytic bound of the average SER. The optimization aims to minimize the sum of the EPs for all users subject to the power constraint, which can be written as

$$\begin{aligned} &\min_{\mathbf{x},\mathbf{p}}\ \mathbf{1}_{2K}^T\mathbf{p} \\ &\text{s.t. } \Pr\Big(\pi+\theta \geq \psi_i(\mathbf{x},n_i) \geq \theta\Big) \leq p_{2i-1}, \quad \forall i = 1,\ldots,K, \\ &\quad \Pr\Big(-\pi-\theta \geq \psi_i(\mathbf{x},n_i) \geq -\theta\Big) \leq p_{2i}, \quad \forall i = 1,\ldots,K, \\ &\quad \|\mathbf{x}\|^2 \leq P, \quad 0 \leq p_j, \quad \forall j = 1,\ldots,2K, \end{aligned} \tag{74}$$

where $\mathbf{p} = (p_1\ p_2\ \ldots\ p_{2K})^T$ is a $2K\times 1$ vector and the sum EPs for all users is defined to be $\mathbf{1}_{2K}^T\mathbf{p}$. Similarly to the approach of Section V, we can rewrite (74) as a function $\mathbf{p}^\star(\cdot)$ for any given $P \geq 0$ such that

$$\begin{aligned} \mathbf{p}^\star(P):\ &\min_{\bar{\mathbf{x}},\mathbf{p}}\ \mathbf{1}_{2K}^T\mathbf{p} \\ &\text{s.t. } -\mathbf{T}\bar{\mathbf{x}} + \mathrm{erf}^{-1}(1-2\mathbf{p}) \leq \mathbf{0}_{2K}, \\ &\quad \|\bar{\mathbf{x}}\|^2 \leq P, \quad 0 \leq p_j \leq 0.5,\ \forall j = 1,\ldots,2K, \end{aligned} \tag{75}$$

which can be expressed as

$$\begin{aligned} &\min_{\bar{\mathbf{x}},\mathbf{q}}\ K - \frac{\mathbf{1}_{2K}^T\mathrm{erf}(\mathbf{q})}{2} \\ &\text{s.t. } -\mathbf{T}\bar{\mathbf{x}} + \mathbf{q} \leq \mathbf{0}_{2K}, \mathbf{0}_{2K} \leq \mathbf{q}, \\ &\quad \|\bar{\mathbf{x}}\|^2 \leq P, \end{aligned} \tag{76}$$

where $\mathrm{erf}^{-1}(\cdot)$ and $\mathrm{erf}(\cdot)$ are elementwise inverse error and error functions and $\mathbf{q}$ is a $2K\times 1$ vector such that $\mathbf{p} = \frac{1}{2} - \frac{1}{2}\mathrm{erf}(\mathbf{q})$.

Remark: Function $\mathrm{erf}(x)$ is concave for $x \geq 0$. This implies that the objective function of (76) is a convex function. Hence, problem (76) is a convex optimization. Furthermore, a feasible point of (68) is also a feasible point of (76). Thus it can be shown that (76) contains an interior point. By Slater's condition, the strong duality holds for (76).

By multiplying the objective function by a constant, the optimal solution of (76) will remain unchanged. Hence, we can equivalently solve the following problem

$$\begin{aligned} &\min_{\bar{\mathbf{x}},\mathbf{q}}\ \sqrt{\pi}\Big(K - \frac{\mathbf{1}_{2K}^T\mathrm{erf}(\mathbf{q})}{2}\Big) \\ &\text{s.t. } -\mathbf{T}\bar{\mathbf{x}} + \mathbf{q} \leq \mathbf{0}_{2K}, \mathbf{0}_{2K} \leq \mathbf{q}, \|\bar{\mathbf{x}}\|^2 \leq P. \end{aligned} \tag{77}$$

The Lagrangian of (77) is given by

$$\begin{aligned} L(\bar{\mathbf{x}},\mathbf{q},\mathbf{u},\mathbf{v},r) = \sqrt{\pi}\Big(K - \frac{\mathbf{1}_{2K}^T\mathrm{erf}(\mathbf{q})}{2}\Big) + \mathbf{u}^T(-\mathbf{T}\bar{\mathbf{x}} + \mathbf{q}) \\ -\mathbf{v}^T\mathbf{q} + r(\|\bar{\mathbf{x}}\|^2 - P), \end{aligned} \tag{78}$$

where $\mathbf{u}$ and $\mathbf{v}$ are $2K\times 1$ unknown variable vectors.

Remark: If $v_i^\star \neq 0$, then Slater's condition leads to $q_i^\star = 0$ and implies that $p_i^\star = 0.5$.

Taking the derivative of (78) with respect to $\bar{\mathbf{x}}$ and setting to zeros, we can write $\bar{\mathbf{x}}^\star$ as

$$\bar{\mathbf{x}}^\star = \frac{1}{2r^\star}\mathbf{T}^T\mathbf{u}^\star. \tag{79}$$

Furthermore, if $\bar{\mathbf{x}}^\star$ is an optimal solution of transmit signal in (77), then using the similar argument in [6] it can be shown that

$$\|\bar{\mathbf{x}}^\star\|^2 = P. \tag{80}$$

Using (80) and (79), we can express $r^\star$ as

$$r^\star = \frac{\|\mathbf{T}^T\mathbf{u}^\star\|}{2\sqrt{P}}. \tag{81}$$

Thus, the optimal solution of transmit signal $\bar{\mathbf{x}}^\star$ for (77) can be rewritten as

$$\bar{\mathbf{x}}^\star = \frac{\sqrt{P}}{\|\mathbf{T}^T\mathbf{u}^\star\|}\mathbf{T}^T\mathbf{u}^\star. \tag{82}$$

Taking the derivative of (78) with respect to $\mathbf{q}$, and setting to zero, we reach $-\mathrm{e}^{-\mathbf{q}^{\star 2}} + \mathbf{u}^\star - \mathbf{v}^\star = \mathbf{0}_{2K}$ or equivalently,

$$\mathbf{q}^\star = \sqrt{-\ln(\mathbf{u}^\star - \mathbf{v}^\star)}. \tag{83}$$

Using (82) and (83), the dual problem of (77) can be reformulated as

$$\begin{aligned}\max_{\mathbf{u},\mathbf{v}}\ & \sqrt{\pi}K - \int_{\mathbf{u}-\mathbf{v}}^{\mathbf{1}_{2K}} \mathbf{1}_{2K}^T\sqrt{-\ln\mathbf{z}}\,d\mathbf{z} - \sqrt{P}\|\mathbf{T}^T\mathbf{u}\| \\ \text{s.t. }& \mathbf{0}_{2K} \leq \mathbf{u},\quad \mathbf{0}_{2K} \leq \mathbf{v},\ \mathbf{0}_{2K} \leq \mathbf{u}-\mathbf{v} \leq \mathbf{1}_{2K},\end{aligned} \tag{84}$$

where

$$\int_\zeta^1 \sqrt{-\ln x}\,dx = \frac{\sqrt{\pi}}{2}\,\mathrm{erf}\Big(\sqrt{-\ln\zeta}\Big) - \zeta\sqrt{-\ln\zeta} \tag{85}$$

using the integration by parts [58]. We can rewrite (84) as a corresponding standard minimization problem:

$$\min_{\mathbf{0}_{2K}\leq\mathbf{u},\mathbf{v}}\ f(\mathbf{u},\mathbf{v}) \quad \text{s.t. } \mathbf{0}_{2K} \leq \mathbf{u}-\mathbf{v} \leq \mathbf{1}_{2K}, \tag{86}$$

where

$$f(\mathbf{u},\mathbf{v}) \triangleq -\sqrt{\pi}K + \int_{\mathbf{u}-\mathbf{v}}^{\mathbf{1}_{2K}} \mathbf{1}_{2K}^T\sqrt{-\ln\mathbf{z}}\,d\mathbf{z} + \sqrt{P}\|\mathbf{T}^T\mathbf{u}\|.$$

To solve (86), we need to show the objective function of (86) is convex. Note that for the double derivative

$$\Big(\int_\zeta^1 \sqrt{-\ln x}dx\Big)'' = \Big(2\zeta\sqrt{-\ln\zeta}\Big)^{-1} \geq 0. \tag{87}$$

Thus it is a convex function. Since norm is a convex function and $f(\mathbf{u},\mathbf{v})$ is a sum of convex functions, it is also convex. Therefore, problem (86) is a convex optimization problem. Putting (82), (83) into (77), we can reformulate (77) as

$$\begin{aligned}\min_{\mathbf{u},\mathbf{v}}\ & \sqrt{\pi}\Big(K - \frac{\mathbf{1}_{2K}^T\mathrm{erf}(\sqrt{-\ln(\mathbf{u}-\mathbf{v})})}{2}\Big) \\ \text{s.t. }& -\bigtriangledown\mathbf{f}(\mathbf{u},\mathbf{v}) \leq \mathbf{0}_{2K}\end{aligned} \tag{88}$$

where the gradient of $f(\mathbf{u},\mathbf{v})$ in (86) are given by

$$\bigtriangledown\mathbf{f}(\mathbf{u},\mathbf{v}) = \begin{bmatrix} -\sqrt{-\ln(\mathbf{u}-\mathbf{v})} + \dfrac{\sqrt{P}}{\|\mathbf{T}^T\mathbf{u}\|}\mathbf{T}\mathbf{T}^T\mathbf{u} \\ \sqrt{-\ln(\mathbf{u}-\mathbf{v})} \end{bmatrix}. \tag{89}$$

Hence, we need to ensure that $\bigtriangledown\mathbf{f}(\mathbf{u}^\star,\mathbf{v}^\star) \geq \mathbf{0}_{2K}$. To efficiently compute (86), similarly to the approach in Section V we propose to use the barrier method to obtain the optimal solution. Let

$$\begin{aligned}\phi(\mathbf{u},\mathbf{v}) =& -\mathbf{1}_{2K}^T\ln(\mathbf{u}) - \mathbf{1}_{2K}^T\ln(\mathbf{v}) - \mathbf{1}_{2K}^T\ln(\mathbf{u}-\mathbf{v}) \\ & - \mathbf{1}_{2K}^T\ln(\mathbf{1}_{2K}-\mathbf{u}+\mathbf{v})\end{aligned} \tag{90}$$

be the logarithmic barrier function. For $s > 0$, define $\mathbf{u}^\star(s)$ and $\mathbf{v}^\star(s)$ as the solution of

$$\min_{\mathbf{u},\mathbf{v}}\ sf(\mathbf{u},\mathbf{v}) + \phi(\mathbf{u},\mathbf{v}). \tag{91}$$

The barrier method for solving (75) is summarized as Algorithm 4. As the barrier method yields globally optimal solutions, and similar to the barrier method in Algorithm 2, Algorithm 4 also gives globally optimal solutions. Our results in the following section show that Algorithm 4 provides the best SER performance amongst the proposed optimizations.

Algorithm 4 Efficient Barrier Method Algorithm to Solve (75)

Input: $\{\mathbf{h}_i\}_{i=1}^K, \{b_i\}_{i=1}^K, P_0, \sigma, \mu$
Output: The optimal solution $(\bar{\mathbf{x}}^\star, \bar{\mathbf{p}}^\star)$ of problem (75)
repeat
  Compute $(\mathbf{u}^\star(s), \mathbf{v}^\star(s))$ of (91) ;
  Set $s = \mu s$;
until $\|\mathbf{u}^\star(s) - \mathbf{u}^\star(s-1)\|^2 + \|\mathbf{v}^\star(s) - \mathbf{v}^\star(s-1)\|^2 < \Delta_t^2$ and $\min\bigtriangledown\mathbf{f}(\mathbf{u}^\star(s),\mathbf{v}^\star(s)) > -\Delta_t$;
Output

$$\bar{\mathbf{x}}^\star = \frac{\sqrt{P_0}}{\|\mathbf{T}^T\mathbf{u}^\star(s)\|}\mathbf{T}^T\mathbf{u}^\star(s)$$

$$\bar{\mathbf{p}}^\star = \frac{1}{2} - \frac{\mathrm{erf}\Big(\sqrt{-\ln\big(\mathbf{u}^\star(s) - \mathbf{v}^\star(s)\big)}\Big)}{2};$$

VII. Simulations

In our simulations, we consider a downlink beamforming network with $N = 10$ antennas, while it is intuitive that the benefits shown extend to different numbers of antennas. In line with our benchmark techniques [6], [40] we assume an uncoded transmission, while it would be interesting to examine the joint design of precoding and forward error correction (FEC) for practical modulation schemes as the focus of future work. The system with QPSK modulation is considered, i.e., $\theta = \pi/4$, while it is obvious that the benefit of the proposed approaches extend to BPSK, or higher order PSK modulation, similarly to the approaches in [40] and [41]. The circularly symmetric complex Gaussian noise n_i is complex zero-mean with the variance $\sigma^2 = 1$. Let ω_i be a uniformly distributed random number between $-\pi/2$ and $\pi/2$. Then the

downlink channel between the BS and ith user are modeled as

$$\mathbf{h}_i = \left[1, e^{j\pi \sin\omega_i}, \ldots, e^{j\pi(N-1)\sin\omega_i}\right]^T, \qquad (92)$$

i.e., the identical path loss line-of-sight channel model is assumed [26]. All results are averaged over 10000 Monte Carlo runs. The maximum iteration number $i_{\max} = 1000$ and error tolerance $\Delta_t = 10^{-4}$ are used in Algorithm 1. For the barrier methods, we set $\mu = 100$ and the maximum number of inner iterations in the gradient descent method is set to $i_{GD} = 100$.

In the simulations, we omit the power minimization approaches and focus on the SINR-, SNR- and EP- based optimizations that can be compared by SER results, as a common metric between constructive interference-based and conventional optimizations for a given power. It is intuitive however, that the symmetrical versions of the problems where power is minimized subject to our new SNR/detection region/error probability constraints, similarly outperform conventional power minimization as per the benefits of our relaxed optimization regions. Based on our analysis in Section V, since the detection-region based approach of (21) and the worst user EP approach of (68) are equivalent, in the following simulations, we only consider the detection-region based approach. We compare the following techniques:

- 'SINR Balancing [6]' refers to the conventional SINR balancing problem in [6];
- 'Gradient descent DRB ($\cong$ [40])' stands for using the gradient descent approach to solve the decision-region based optimization in Algorithm 3 and problem (21), which is equivalent to (10) proposed in [40];
- 'CIMM [41]' refers to the interference exploitation approach of [41];
- 'Barrier method DRB' refers to use the barrier method in Algorithm 3 to solve the detection-region based problem (21);
- 'Barrier method sum EPs' refers to the barrier method in Algorithm 4 to solve (75);
- 'Analyt-DRB' and 'Analyt-sum EPs' refer to the analytical bounds for using the barrier method of (68) and (75), respectively;
- 'Analyt-sum EPs' is the analytic bound of the average SER.

A. Complexity

Fig. 2 compares the trend of the average execution time of our proposed methods and the gradient descent detection-region based method for different number of users with a transmit SNR of $\frac{E_b}{\sigma^2} = 20$dB, where E_b is the energy per transmitted bit. As shown in Fig. 2, when the number of users is small, the average execution time of the gradient descent detection-region based method is faster than the both barrier methods of detection-region based approach and sum EPs approach. Nonetheless, when the number of users increases, the barrier detection-region based approach has a higher computational efficiency than the gradient descent detection-region based approach.

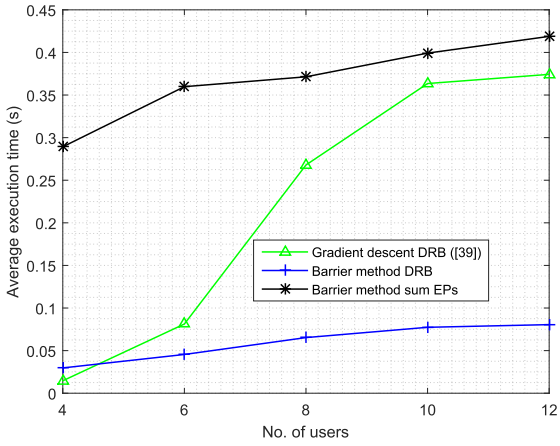

Fig. 2. Average execution time versus number of users with $N = 10$, and SNR $= 20$dB.

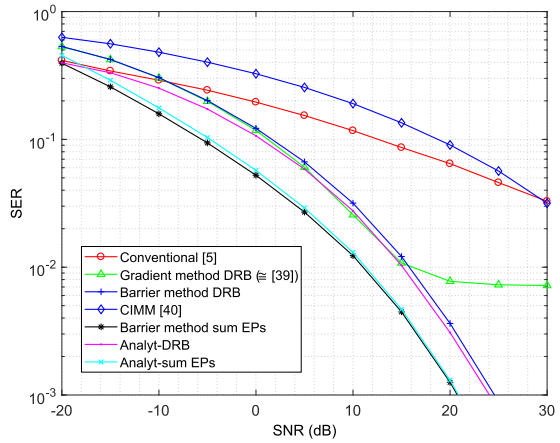

Fig. 3. SER performance versus SNR with $N = 10$, and $K = 10$.

B. Performance Comparison

Fig. 3-4 compare the SER performance for the different techniques. In Fig. 3, we fix the number of users and compare both experimental and analytic SER performance of all approaches versus the SNR for $K = 10$. It can be seen from these figures that the the sum EPs approach given in (75) outperforms the detection-region based (DRB) approach, the conventional method of (5), and the CIMM scheme of [41] in terms of the experimental SER performance. As per our derivations above we reiterate that the DRB approach is equivalent to the worst EP approach, which is still outperformed by the sum EP optimization. Indeed, we have observed that while the worst EP approach provides a slightly better worst EP compared to the sum EP approach, the EP obtained for the rest of the users (second worst onwards) is significantly inferior to the sum EP approach. Accordingly the average EP obtained (the one shown in our results) is typically lower for the sum EP approach. We also notice that the detection-region based technique outperformns the technique in [40], and CIMM in [41] at higher transmit power. Importantly, it can be observed that our analytic SER performance calculations match the simulated SER results. Furthermore, the proposed sum EPs approach achieves the analytic bound of the average

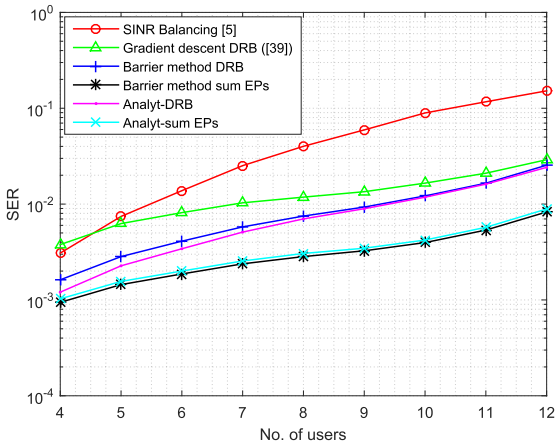

Fig. 4. SER performance versus number of users with $N = 10$, and SNR$=$ 20dB.

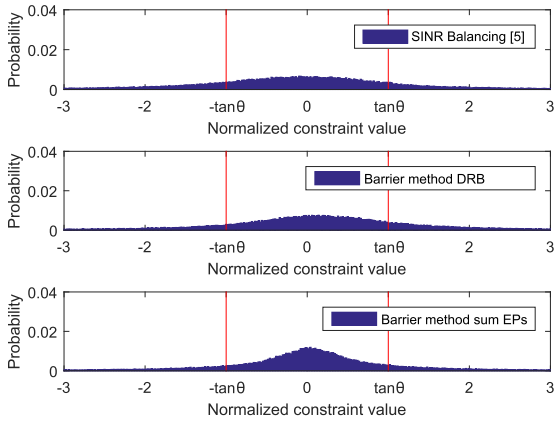

Fig. 5. Histogram of normalized constraint value with $N = 10$, $K = 10$ and SNR $= 5$dB.

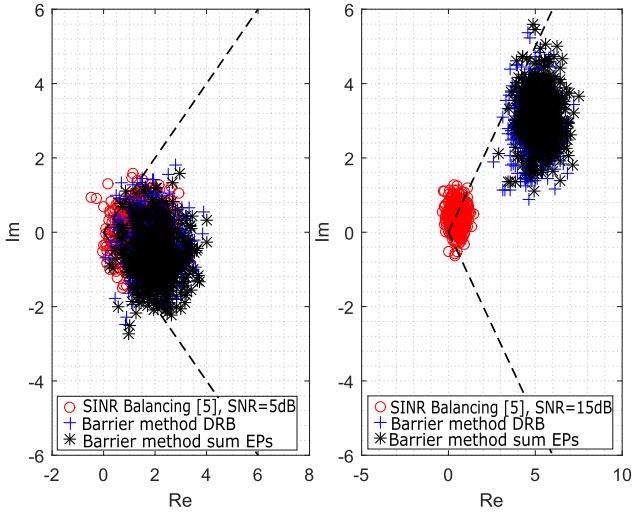

Fig. 6. Distribution of received signals on complex plane where $N = 10$, and $K = 10$ with SNR$=$ 5dB and SNR $=$ 15dB, respectively.

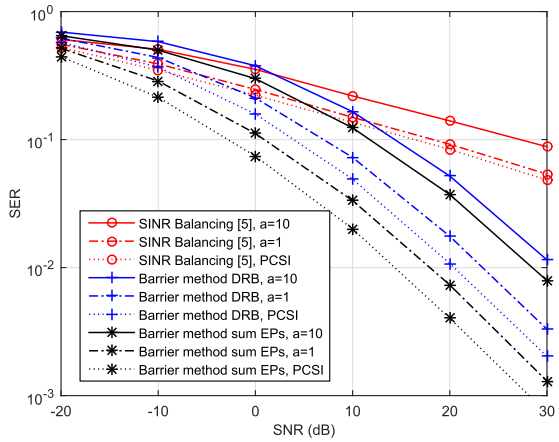

Fig. 7. SER performance versus SNR with $N = 10$, and $K = 10$, imperfect CSI.

SER performance. The gradient method detection-region based approach is characterized by an error floor as it is not guaranteed to converge. In Fig. 4, we illustrate both simulated and analytic SER performance for increasing numbers of users when we set the transmit SNR to be 20dB. We observe that the SER performance of our proposed approaches are better than the conventional approach of [6] and the gradient descent approach given in [40], respectively. The proposed sum EPs approach using the barrier method has the best performance.

In Fig. 5 and Fig. 6, we look at the distribution of the received signals. We introduce the normalized constraint value

$$\eta_i = \begin{cases} \dfrac{\mathrm{Im}(y_i b_i^*)}{\mathrm{Re}(y_i b_i^*)} & \mathrm{Re}(y_i b_i^*) > 0, \\ \infty & \text{otherwise}, \end{cases} \tag{93}$$

As a measure of the resulting deviation from the angle of the desired symbol b_i, to evaluate the performance of the different approaches. Fig. 5 displays the histograms of η_i with $K = 10$ and SNR$=$ 5dB. According to Lemma 1, the receive signal can be correctly classified if it is within the region between $-\tan\theta$ and $\tan\theta$. As can be observed from Fig. 5, the conventional and the worst user EP approaches satisfy about 75% and 80% of the normalized constraints, respectively. However, the sum EPs approach achieves about 90% of the normalized constraints with normal-like distribution. Fig. 6 depicts the distribution of the received signals on the modulation constellation using different techniques with SNR$=$ 5dB and SNR$=$ 15dB. Here, we set the transmit symbol to 1. We observe from these figures that the received signals of our proposed methods can better center the received symbol into the correct detective region compared to the conventional method. We also notice that when the power increases, our techniques can shift the received signals further away from the decision threshold which further improves the error rate performance.

C. Imperfect CSI

Finally, in Fig. 7 we illustrate the comparison of our proposed schemes and the conventional scheme in [6] under imperfect CSI. To keep the CSI imperfections generic, we model the estimated CSI as [15], [16]

$$\hat{\mathbf{h}}_i^T = \mathbf{h}_i^T + \mathbf{e}_i \tag{94}$$

where $\mathbf{e}_i \sim \mathcal{CN}(0, a\left(\frac{P}{\sigma^2}\right)^{-1}\mathbf{I})$, and a is a constant. It can be seen in the results that the performance of both proposed and conventional schemes deteriorates with imperfect CSI, while the performance gains of the proposed w.r.t. conventional beamforming persist. We note however, that existing CSI-robust approaches [31] can be adapted to the proposed optimization, to further improve performance against CSI errors. We designate this as the focus of our future work.

VIII. Conclusion

In this paper, we exploit constructive interference by making use of CSI and data information jointly. We propose beamforming optimizations for QoS based on the detection regions of the symbol constellation, in terms of the worst user EP, and sum EPs, respectively. The detection-region based and the worst user EP downlink beamforming are shown to be equivalent problems. Using the sum EPs approach, we obtain an analytic bound of the average SER performance. Simulation results have demonstrated that our proposed methods have substantially improved performance compared to conventional downlink beamforming and constructive interference-based optimizations. Our future work will focus on reducing the complexity of the algorithm of the sum EPs approach by providing a heuristic algorithm. Other interesting research topics are to jointly optimize beamforming and FEC for interference exploitation, and to develop CSI-robust approaches as detailed above. Communication theoretic future work will focus on deriving modulation-dependent sum rate bounds for the concept of interference exploitation, using finite constellation sum rate analysis.

Appendix

A. Proof of Corollary 1

The dual Lagrange function is given by

$$\mathcal{L}(\kappa_i, n_i) = -\,|\operatorname{Im}(\tilde{y}_i)| + \operatorname{Re}(\tilde{y}_i)\tan\theta + \kappa_i(\|n_i\|^2 - \Gamma^2\sigma^2), \tag{95}$$

where $\tilde{y}_i = b_i^*(\mathbf{h}_i^T\tilde{\mathbf{x}} + n_i)$ and $\kappa_i \geq 0$. We define $n_i \triangleq n_{Ri} + in_{Ii}$, and $b_i \triangleq b_{Ri} + ib_{Ii}$. By using chain rule [58] and setting $\frac{\partial\mathcal{L}}{\partial n_{Ri}} = 0$ and $\frac{\partial\mathcal{L}}{\partial n_{Ii}} = 0$, we get

$$b_{Ri}\tan\theta + b_{Ii}\alpha_i + 2\kappa_i^\star n_{Ri}^\star = 0, \tag{96a}$$

$$-b_{Ri}\alpha_i + b_{Ii}\tan\theta + 2\kappa_i^\star n_{Ii}^\star = 0, \tag{96b}$$

where $a^\star$ is the optimal value of a, and $\alpha_i = \operatorname{Im}(\tilde{y}_i)/|\operatorname{Im}(\tilde{y}_i)|$. Suppose $\kappa_i^\star = 0$. Then (96) implies that $b_{Ri} = b_{Ii} = 0$, which leads to the contradiction. Thus it is always true that $\kappa_i^\star > 0$ and

$$\|n_i^\star\|^2 = \Gamma^2\sigma^2 \tag{97}$$

by the complementary slackness [25]. By (96), we obtain

$$n_{Ri}^\star = -(b_{Ri}\tan\theta + b_{Ii}\alpha_i)/2\kappa_i^\star, \tag{98a}$$

$$n_{Ii}^\star = (b_{Ri}\alpha_i - b_{Ii}\tan\theta)/2\kappa_i^\star. \tag{98b}$$

Putting (98) into (97), we can write (97) as

$$\left(\frac{b_{Ri}\tan\theta + b_{Ii}\alpha_i}{2\kappa_i^\star}\right)^2 + \left(\frac{b_{Ri}\alpha_i - b_{Ii}\tan\theta}{2\kappa_i^\star}\right)^2 = \Gamma^2\sigma^2. \tag{99}$$

Since b_i is an unit power symbol, we can express (99) as

$$\frac{1+\tan^2\theta}{4\kappa_i^{\star 2}} = \Gamma^2\sigma^2. \tag{100}$$

Thus, we have the following relation:

$$\kappa_i^\star = \frac{1}{2\Gamma\sigma\cos\theta}. \tag{101}$$

We put (101) back into (98), then we have

$$n_{Ri}^\star = -(b_{Ri}\tan\theta + b_{Ii}\alpha_i)\Gamma\sigma\cos\theta, \tag{102a}$$

$$n_{Ii}^\star = (b_{Ri}\alpha_i - b_{Ii}\tan\theta)\Gamma\sigma\cos\theta. \tag{102b}$$

Substituting (102) into problem (19), we reformulate the constraint (19a) as

$$\begin{aligned}
&\max_{\|n_i\|\leq\Gamma\sigma} |\operatorname{Im}(\tilde{y}_i))| - \operatorname{Re}(\tilde{y}_i)\tan\theta \\
&\quad= \alpha_i\operatorname{Im}(b_i^*\mathbf{h}_i^T\tilde{\mathbf{x}}) + \alpha_i\operatorname{Im}(b_i^*n_i^\star) \\
&\qquad- \operatorname{Re}(b_i^*n_i^\star)\tan\theta - \operatorname{Re}(b_i^*\mathbf{h}_i^T\tilde{\mathbf{x}})\tan\theta \\
&\quad= \alpha_i\operatorname{Im}(b_i^*\mathbf{h}_i^T\tilde{\mathbf{x}}) - n_{Ri}^\star(b_{Ri}\tan\theta + b_{Ii}\alpha_i) \\
&\qquad+ n_{Ii}^\star(b_{Ri}\alpha_i - b_{Ii}\tan\theta) - \operatorname{Re}(b_i^*\mathbf{h}_i^T\tilde{\mathbf{x}})\tan\theta \\
&\quad= |\operatorname{Im}(b_i^*\mathbf{h}_i^T\tilde{\mathbf{x}})| + \Gamma\sigma/\cos\theta - \operatorname{Re}(b_i^*\mathbf{h}_i^T\tilde{\mathbf{x}})\tan\theta,
\end{aligned} \tag{103}$$

where $\operatorname{Im}(\tilde{y}_i)$ and $\operatorname{Re}(b_i^*\mathbf{h}_i^T\tilde{\mathbf{x}})$ have the same sign as the noise cannot dominate the received signal. ■

B. Proof of Corollary 2

Since $(\Gamma_0, \mathbf{x}_P^\star(\Gamma_0))$ is a candidate solution of (29), it implies that $\Gamma^\star(P^\star(\Gamma_0)) \geq \Gamma_0$. Suppose $\Gamma^\star(P^\star(\Gamma_0)) > \Gamma_0$. Let $\Gamma^\star(P^\star(\Gamma_0)) = \beta\Gamma_0$ for some $\beta > 1$. By (21) and (52), it can guarantee that

$$|\operatorname{Im}(b_i^*\mathbf{h}_i^T\mathbf{x}_P^\star(\Gamma_0))| + \frac{\beta\Gamma_0\sigma}{\cos\theta} \leq \operatorname{Re}(b_i^*\mathbf{h}_i^T\mathbf{x}_P^\star(\Gamma_0))\tan\theta, \tag{104}$$

$$\|\mathbf{x}_P^\star(\Gamma_0)\|^2 = P^\star(\Gamma_0), \quad \forall i. \tag{105}$$

Let $\hat{\mathbf{x}} = \mathbf{x}_P^\star(\Gamma_0)/\beta$. Then we can rewrite as

$$|\operatorname{Im}(b_i^*\mathbf{h}_i^T\hat{\mathbf{x}})| + \Gamma_0\sigma/\cos\theta \leq \operatorname{Re}(b_i^*\mathbf{h}_i^T\hat{\mathbf{x}})\tan\theta, \quad \forall i, \tag{106}$$

$$\|\hat{\mathbf{x}}\|^2 = P^\star(\Gamma_0)/\beta^2, \tag{107}$$

which contradicts that $P^\star(\Gamma_0)$ is the minimum power for the given Γ_0. Similarly, we can use the same approach to show the second half of Corollary 2. ■

C. Proof of Corollary 3

Let Γ_0 be any given positive number. Since (21) has a nontrivial solution, we obtain a solution $(\Gamma^\star(1), \mathbf{x}_\Gamma^\star(1))$ of (21) for $P = 1$. Then there exists P_0 such that

$$\Gamma_0 = \sqrt{P_0}\Gamma^\star(1) = \Gamma^\star(P_0). \tag{108}$$

Then by Corollary 2, we have

$$P^\star(\Gamma_0) = P^\star(\Gamma^\star(P_0)) = P_0, \tag{109}$$

$$\mathbf{x}_P^\star(\Gamma_0) = \mathbf{x}_P^\star(\Gamma^\star(P_0)) = \mathbf{x}_\Gamma^\star(P_0) = \sqrt{P_0}\mathbf{x}_\Gamma^\star(1). \tag{110}$$

This shows that problem (29) is feasible for the given Γ_0. ■

REFERENCES

[1] K. L. Law and C. Masouros, "Constructive interference exploitation for downlink beamforming based on noise robustness and outage probability," in *Proc. IEEE Int. Conf. Acoust., Speech Signal Process. (ICASSP)*, Mar. 2016, pp. 3291–3295.

[2] E. Dahlman, S. Parkvall, and J. Skold, *4G: LTE/LTE-Advanced for Mobile Broadband*. Amsterdam, The Netherlands: Elsevier, 2011.

[3] A. F. Molisch, *Wireless Communications*. Hoboken, NJ, USA: Wiley, 2011.

[4] A. B. Gershman, N. D. Sidiropoulos, S. Shahbazpanahi, M. Bengtsson, and B. Ottersten, "Convex optimization-based beamforming," *IEEE Signal Process. Mag.*, vol. 27, no. 3, pp. 62–75, May 2010.

[5] F. Rashid-Farrokhi, K. J. R. Liu, and L. Tassiulas, "Transmit beamforming and power control for cellular wireless systems," *IEEE J. Sel. Areas Commun.*, vol. 16, no. 8, pp. 1437–1450, Oct. 1998.

[6] M. Schubert and H. Boche, "Solution of the multiuser downlink beamforming problem with individual SINR constraints," *IEEE Trans. Veh. Technol.*, vol. 53, no. 1, pp. 18–28, Jan. 2004.

[7] M. Bengtsson and B. Ottersten, "Optimal downlink beamforming using semidefinite optimization," in *Proc. Annu. Allerton Conf. Commun., Control Comput.*, vol. 37, 1999, pp. 987–996.

[8] M. Bengtsson and B. Ottersten, "Optimal and suboptimal transmit beamforming," in *Handbook of Antennas in Wireless Communications*. Boca Raton, FL, USA: CRC Press, 2001.

[9] A. Wiesel, Y. C. Eldar, and S. Shamai (Shitz), "Linear precoding via conic optimization for fixed MIMO receivers," *IEEE Trans. Signal Process.*, vol. 54, no. 1, pp. 161–176, Jan. 2006.

[10] J. Choi, "Downlink multiuser beamforming with compensation of channel reciprocity from RF impairments," *IEEE Trans. Commun.*, vol. 63, no. 6, pp. 2158–2169, Jun. 2015.

[11] M. Costa, "Writing on dirty paper (Corresp.)," *IEEE Trans. Inf. Theory*, vol. 29, no. 3, pp. 439–441, May 1983.

[12] U. Erez, S. Shamai, and R. Zamir, "Capacity and lattice strategies for canceling known interference," *IEEE Trans. Inf. Theory*, vol. 51, no. 11, pp. 3820–3833, Nov. 2005.

[13] C. Windpassinger, R. F. H. Fischer, T. Vencel, and J. B. Huber, "Precoding in multiantenna and multiuser communications," *IEEE Trans. Wireless Commun.*, vol. 3, no. 4, pp. 1305–1316, Jul. 2004.

[14] C. B. Peel, B. M. Hochwald, and A. L. Swindlehurst, "A vector-perturbation technique for near-capacity multiantenna multiuser communication—Part I: Channel inversion and regularization," *IEEE Trans. Commun.*, vol. 53, no. 1, pp. 195–202, Jan. 2005.

[15] A. J. Maurer, J. Jalden, D. Seethaler, and G. Matz, "Vector perturbation precoding revisited," *IEEE Trans. Signal Process.*, vol. 59, no. 1, pp. 315–328, Jan. 2011.

[16] C. Masouros, M. Sellathurai, and T. Ratnarajah, "Vector perturbation based on symbol scaling for limited feedback MISO downlinks," *IEEE Trans. Signal Process.*, vol. 62, no. 3, pp. 562–571, Feb. 2014.

[17] C. Masouros, M. Sellathurai, and T. Ratnarajah, "Maximizing energy efficiency in the vector precoded MU-MISO downlink by selective perturbation," *IEEE Trans. Wireless Commun.*, vol. 13, no. 9, pp. 4974–4984, Sep. 2014.

[18] C. Masouros, M. Sellathurai, and T. Ratnarajah, "Computationally efficient vector perturbation precoding using thresholded optimization," *IEEE Trans. Commun.*, vol. 61, no. 5, pp. 1880–1890, May 2013.

[19] C. Masouros, M. Sellathurai, and T. Ratnarajah, "A low-complexity sequential encoder for threshold vector perturbation," *IEEE Commun. Lett.*, vol. 17, no. 12, pp. 2225–2228, Dec. 2013.

[20] C. Masouros, M. Sellathurai, and T. Ratnarajah, "Interference optimization for transmit power reduction in Tomlinson-Harashima precoded MIMO downlinks," *IEEE Trans. Signal Process.*, vol. 60, no. 5, pp. 2470–2481, May 2012.

[21] A. Garcia-Rodriguez and C. Masouros, "Power-efficient Tomlinson-Harashima precoding for the downlink of multi-user MISO systems," *IEEE Trans. Commun.*, vol. 62, no. 6, pp. 1884–1896, Jun. 2014.

[22] Q. H. Spencer, A. L. Swindlehurst, and M. Haardt, "Zero-forcing methods for downlink spatial multiplexing in multiuser MIMO channels," *IEEE Trans. Signal Process.*, vol. 52, no. 2, pp. 461–471, Feb. 2004.

[23] K.-K. Wong, R. D. Murch, and K. B. Letaief, "A joint-channel diagonalization for multiuser MIMO antenna systems," *IEEE Trans. Wireless Commun.*, vol. 2, no. 4, pp. 773–786, Jul. 2003.

[24] Z.-Q. Luo, W.-K. Ma, A. M.-C. So, Y. Ye, and S. Zhang, "Semidefinite relaxation of quadratic optimization problems," *IEEE Signal Process. Mag.*, vol. 27, no. 3, pp. 20–34, May 2010.

[25] S. Boyd and L. Vandenberghe, *Convex Optimization*. Cambridge, U.K.: Cambridge Univ. Press, 2004.

[26] Y. Huang and D. P. Palomar, "Rank-constrained separable semidefinite programming with applications to optimal beamforming," *IEEE Trans. Signal Process.*, vol. 58, no. 2, pp. 664–678, Feb. 2010.

[27] Y. Huang and D. P. Palomar, "A dual perspective on separable semidefinite programming with applications to optimal downlink beamforming," *IEEE Trans. Signal Process.*, vol. 58, no. 8, pp. 4254–4271, Aug. 2010.

[28] K. Law, X. Wen, M. T. Vu, and M. Pesavento, "General rank multiuser downlink beamforming with shaping constraints using real-valued OSTBC," *IEEE Trans. Signal Process.*, vol. 63, no. 21, pp. 5758–5771, Nov. 2015.

[29] M. B. Shenouda and T. N. Davidson, "Convex conic formulations of robust downlink precoder designs with quality of service constraints," *IEEE J. Sel. Topics Signal Process.*, vol. 1, no. 4, pp. 714–724, Dec. 2007.

[30] N. Vucic and H. Boche, "Robust QoS-constrained optimization of downlink multiuser MISO systems," *IEEE Trans. Signal Process.*, vol. 57, no. 2, pp. 714–725, Feb. 2009.

[31] I. Wajid, M. Pesavento, Y. C. Eldar, and D. Ciochina, "Robust downlink beamforming with partial channel state information for conventional and cognitive radio networks," *IEEE Trans. Signal Process.*, vol. 61, no. 14, pp. 3656–3670, Jul. 2013.

[32] B. K. Chalise, S. Shahbazpanahi, A. Czylwik, and A. B. Gershman, "Robust downlink beamforming based on outage probability specifications," *IEEE Trans. Wireless Commun.*, vol. 6, no. 10, pp. 3498–3503, Oct. 2007.

[33] E. Alsusa and C. Masouros, "Adaptive code allocation for interference management on the downlink of DS-CDMA systems," *IEEE Trans. Wireless Commun.*, vol. 7, no. 7, pp. 2420–2424, Jul. 2008.

[34] C. Masouros and E. Alsusa, "Soft linear precoding for the downlink of DS/CDMA communication systems," *IEEE Trans. Veh. Technol.*, vol. 59, no. 1, pp. 203–215, Jan. 2010.

[35] C. Masouros and E. Alsusa, "Dynamic linear precoding for the exploitation of known interference in MIMO broadcast systems," *IEEE Trans. Wireless Commun.*, vol. 8, no. 3, pp. 1396–1404, Mar. 2009.

[36] C. Masouros, "Correlation rotation linear precoding for MIMO broadcast communications," *IEEE Trans. Signal Process.*, vol. 59, no. 1, pp. 252–262, Jan. 2011.

[37] C. Masouros and T. Ratnarajah, "Interference as a source of green signal power in cognitive relay assisted co-existing MIMO wireless transmissions," *IEEE Trans. Commun.*, vol. 60, no. 2, pp. 525–536, Feb. 2012.

[38] C. Masouros, T. Ratnarajah, M. Sellathurai, C. Papadias, and A. Shukla, "Known interference in the cellular downlink: A performance limiting factor or a source of green signal power?" *IEEE Commun. Mag.*, vol. 51, no. 10, pp. 162–171, Oct. 2013.

[39] G. Zheng, I. Krikidis, C. Masouros, S. Timotheou, D.-A. Toumpakaris, and Z. Ding, "Rethinking the role of interference in wireless networks," *IEEE Commun. Mag.*, vol. 52, no. 11, pp. 152–158, Nov. 2014.

[40] C. Masouros and G. Zheng, "Exploiting known interference as green signal power for downlink beamforming optimization," *IEEE Trans. Signal Process.*, vol. 63, no. 14, pp. 3628–3640, Jul. 2015.

[41] M. Alodeh, S. Chatzinotas, and B. Ottersten, "Constructive multiuser interference in symbol level precoding for the MISO downlink channel," *IEEE Trans. Signal Process.*, vol. 63, no. 9, pp. 2239–2252, May 2015.

[42] P. V. Amadori and C. Masouros, "Interference-driven antenna selection for massive multiuser MIMO," *IEEE Trans. Veh. Technol.*, vol. 65, no. 8, pp. 5944–5958, Aug. 2016.

[43] P. V. Amadori and C. Masouros, "Large scale antenna selection and precoding for interference exploitation," *IEEE Trans. Commun.*, vol. 65, no. 10, pp. 4529–4542, Oct. 2017.

[44] S. M. Razavi and T. Ratnarajah, "Adaptively regularized phase alignment precoding for multiuser multiantenna downlink," *IEEE Trans. Veh. Technol.*, vol. 64, no. 10, pp. 4863–4869, Oct. 2015.

[45] M. P. Daly and J. T. Bernhard, "Directional modulation technique for phased arrays," *IEEE Trans. Antennas Propag.*, vol. 57, no. 9, pp. 2633–2640, Sep. 2009.

[46] T. Hong, M.-Z. Song, and Y. Liu, "Dual-beam directional modulation technique for physical-layer secure communication," *IEEE Antennas Wireless Propag. Lett.*, vol. 10, pp. 1417–1420, 2011.

[47] Y. Ding and V. F. Fusco, "A vector approach for the analysis and synthesis of directional modulation transmitters," *IEEE Trans. Antennas Propag.*, vol. 62, no. 1, pp. 361–370, Jan. 2014.

[48] P. V. Amadori and C. Masouros, "Constant envelope precoding by interference exploitation in phase shift keying-modulated multiuser transmission," *IEEE Trans. Wireless Commun.*, vol. 16, no. 1, pp. 538–550, Jan. 2017.

[49] F. Liu, C. Masouros, P. V. Amadori, and H. Sun, "An efficient manifold algorithm for constructive interference based constant envelope precoding," *IEEE Signal Process. Lett.*, vol. 24, no. 10, pp. 1542–1546, Oct. 2017.
[50] *Evolved Universal Terrestrial Radio Access (E-UTRA); Physical Channels and Modulation*, document 3GPP TS 36.211, V8.2.0 2008-03 Release 8, 2008.
[51] A. Li and C. Masouros, "Exploiting constructive mutual coupling in P2P MIMO by analog-digital phase alignment," *IEEE Trans. Wireless Commun.*, vol. 16, no. 3, pp. 1948–1962, 2017.
[52] M. Alodeh, S. Chatzinotas, and B. Ottersten, "Constructive interference through symbol level precoding for multi-level modulation," in *Proc. Globecom*, Dec. 2015, pp. 1–6.
[53] M. T. Kabir, M. R. A. Khandaker, and C. Masouros, "Interference exploitation in full duplex communications: Trading interference power for both uplink and downlink power savings," *IEEE Trans. Wireless Commun.*, to be published.
[54] M. R. A. Khandaker, C. Masouros, and K.-K. Wong, "Constructive interference based secure precoding: A new dimension in physical layer security," *IEEE Trans. Inf. Forensics Security*, vol. 13, no. 9, pp. 2256–2268, Sep. 2018.
[55] *CVX: Matlab Software for Disciplined Convex Programming, Version 2.1*, CVX Research Inc., Austin, TX, USA, Jun. 2015.
[56] C. T. Kelley, *Iterative Methods for Optimization* (Frontiers in Applied Math Series). Philadelphia, PA, USA: SIAM, 1999.
[57] Y. Nesterov and I. E. Nesterov, *Introductory Lectures on Convex Optimization*. Dordrecht, The Netherlands: Kluwer, 2004.
[58] J. Stewart, *Calculus*. Boston, MA, USA: Cengage Learning, 2007.
[59] G. S. Smith, "A direct derivation of a single-antenna reciprocity relation for the time domain," *IEEE Trans. Antennas Propag.*, vol. 52, no. 6, pp. 1568–1577, Jun. 2004.
[60] F. Rusek *et al.*, "Scaling up MIMO: Opportunities and challenges with very large arrays," *IEEE Signal Process. Mag.*, vol. 30, no. 1, pp. 40–60, Jan. 2013.
[61] S. K. Mohammed and E. G. Larsson, "Per-antenna constant envelope precoding for large multi-user MIMO systems," *IEEE Trans. Commun.*, vol. 61, no. 3, pp. 1059–1071, Mar. 2013.

Ka Lung Law (M'09) was born in Hong Kong in 1979. He received the B.Sc. degree in computer science from the University of Melbourne, Melbourne, Australia, in 2002, the B.Sc. degree in mathematics from the University of Illinois at Urbana–Champaign in 2003, and the Ph.D. degree in mathematics with computational science and engineering option from the Department of Mathematics, University of Illinois at Urbana–Champaign, in 2008. He has held research positions at the Technische Universität, Darmstadt, Germany, and the University College London, U.K. He is currently a Senior Algorithmic Software Engineer with Huawei Technologies, Hangzhou, China. His research interests mainly include convex optimization in signal processing and wireless communications, adaptive beamforming with higher order space–time coding in MIMO communication system, and multidimensional signal processing for FIR filter banks.

Christos Masouros (SM'14) received the Diploma degree in electrical and computer engineering from the University of Patras, Greece, in 2004, and the M.Sc. (research) and Ph.D. degrees in electrical and electronic engineering from The University of Manchester, U.K., in 2006 and 2009, respectively. In 2008, he was a Research Intern with Philips Research Labs, U.K. From 2009 to 2010, he was a Research Associate with the University of Manchester, and from 2010 to 2012, he was a Research Fellow with Queen's University Belfast. He has held a Royal Academy of Engineering Research Fellowship from 2011 to 2016. He is currently an Associate Professor with the Communications and Information Systems Research Group, Department Electrical and Electronic Engineering, University College London. His research interests lie in the field of wireless communications and signal processing with particular focus on green communications, large scale antenna systems, cognitive radio, and interference mitigation techniques for MIMO and multicarrier communications. He was a recipient of the Best Paper Award at the IEEE GlobeCom 2015 Conference. He was a Guest Editor of the IEEE JOURNAL ON SELECTED TOPICS IN SIGNAL PROCESSING issues Exploiting Interference Towards Energy Efficient and Secure Wireless Communications and Hybrid Analog/Digital Signal Processing for Hardware-Efficient Large Scale Antenna Arrays. He has been recognized as an Exemplary Editor of the IEEE COMMUNICATIONS LETTERS and an Exemplary Reviewer of the IEEE TRANSACTIONS ON COMMUNICATIONS. He is an Editor of the IEEE TRANSACTIONS ON COMMUNICATIONS and an Associate Editor of the IEEE COMMUNICATIONS LETTERS.